

PHOTOABLATION WITH THE FREE-ELECTRON LASER BETWEEN 10 AND 15 μm IN BIOLOGICAL SOFT TISSUE (CORNEA)

Rudolf Walker,[†] Manfred Ostertag,^{†‡} Alexander F. G. van der Meer,^{*} Thomas Bende,[†] Karl C. Schmiedt,[†] and Benedikt Jean[†]

[†]University Eye Hospital, Dept. I, Division Experim. Ophthalmic Surgery, D-72072 Tübingen, Germany; [‡]Vanderbilt University, Dept. of Physics, Nashville, Tennessee 37235; ^{*}FOM Institut for Plasmaphysics, 3430 BE Nieuwegein, The Netherlands

(Paper JBO-082 received Mar. 25, 1996; revised manuscript received Nov. 5, 1996; accepted for publication Feb. 10, 1997.)

ABSTRACT

The ablation depth and collateral thermal damage for pulsed infrared photoablation as a function of wavelength with the free-electron laser (FEL) at 10.1, 11.8, 12.8, and 14.5 μm wavelengths is investigated. FEL data are compared with the *blow-off* and the *continuous* ablation models. Porcine cadaver corneas were used as target material. [Ablation depth per pulse as well as collateral thermal damage (extension of eosinophilic zone at the excision base beyond the irradiated surface) were measured by histologic micrometry.] The experimental data are compared with theoretical calculations for both models. At low water absorption (10.1 μm) the additional absorption of the cornea was taken into account. FEL data were: energy per pulse between 15.6 and 17.8 mJ, ablation zone around 0.2 mm², and pulse length 4 μs (macropulse). In this wavelength range an effective photoablation of biological materials with a high water content can be achieved. The measured FEL data of ablation depth fail to confirm the *blow-off* model; they are 3 to 5 times higher than predicted. However, they are in agreement with the *continuous* ablation model, describing ablation depth sufficiently well ($\pm 10\%$). The wavelength range from 11.8 to 14.5 μm is dominated by water absorption; here the ablation depth depends on the water absorption coefficient only, if other parameters are kept constant. At a 10.1 μm wavelength, collagen absorption contributes to the overall absorption of corneal tissue. The ablation depth can only be described by the *continuous* ablation model; however, the collateral thermal damage pattern can be described by both models (deviation of data $\pm 10\text{--}25\%$). © 1997 Society of Photo-Optical Instrumentation Engineers. [S1083-3668(97)00402-4]

Keywords laser photoablation; ablation depth; thermal damage; free-electron laser; cornea.

1 INTRODUCTION

Photoablation experiments in corneas in the near- and midinfrared wavelength range have been performed by many groups (Tm:YAG laser, 2.02 μm ;¹ Er:YAG laser, 2.94 μm ;² CTE:YAG laser, 2.69 μm ;³ Er:YSGG laser, 2.79 μm ;⁴ and CO₂ laser, 10.6 μm ⁵). However, no data were available beyond the 10.6- μm laser wavelength. The water absorption spectrum shows (Figure 1) that wavelengths between 12 and 20 μm have an absorption coefficient higher than 10³ cm⁻¹; i.e., higher than the absorption coefficient at 10.6 μm (a CO₂ laser wavelength successfully used for ablation of soft tissue). Owing to the high water content of the cornea (>80%), effective ablation was expected. The free-electron laser FELIX at the FOM Institut for Plasma Physics in Nieuwegein, The Netherlands⁶ emits laser radiation between 5 and 110 μm and was thus used for the first systematic investigation of ablation depth per pulse and collateral damage in the cornea for wavelengths beyond 10.6 μm . The experimental results were compared with commonly used ablation models.

2 MATERIALS AND METHODS

Experiments were performed at 10.1-, 11.8-, 12.8-, and 14.5- μm wavelengths; the corresponding water absorption coefficients (data taken from Hale and Querry⁷) are 0.7 $\times 10^3$ cm⁻¹, 1.9 $\times 10^3$ cm⁻¹, 2.8 $\times 10^3$ cm⁻¹, and 3.3 $\times 10^3$ cm⁻¹. Spectroscopic water data shown in Figure 2 were taken from Hale and Querry, and spectroscopic measurements on cornea matrix (dried and fragmented cornea) were done at the Chemical Institute in Tübingen. Ninety-six photoablative incisions were performed on 12 porcine corneas at these four different wavelengths. The setup is shown in Figure 3. A plane and a spherical mirror (focus length=30 cm) were used to focus the beam. Ten pulses were applied for each ablation. The corneas were used within 24 h postmortem; epithelium was debrided immediately before photoablation. The energy per pulse was 17.8 mJ at 10.1 μm , 17.6 mJ at 11.8 μm , 16.5 mJ at 12.8 μm , and 15.6 mJ at 14.5 μm wavelengths. It was monitored with a pyroelectric detector located in a diagnostic sta-

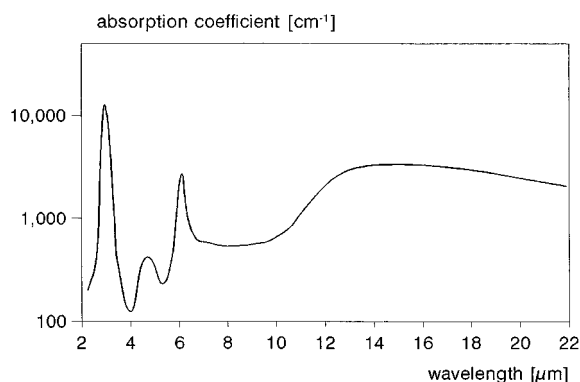


Fig. 1 Absorption coefficient of water in the wavelength range from 2 to 22 μm .⁷

tion and using a fraction of the FEL output for on-line control. The pyroelectric detector was calibrated against an absolute energy meter (Gentec EM 1, Canada) for all wavelengths used. The ablation zone was about 0.2 mm². The spot size was estimated by measuring the ablation zone diameter several times with a sliding caliper immediately after ablation. The laser pulse length (macropulse) was 4 μs . The corneas were fixed on a sample holder.

In order to avoid misleading measurements due to tissue shrinkage during histological preparation, the thickness of the corneas was measured before ablation using a pachymeter (sonogage corneo gage II) and afterward by histologic micrometry of the fixed samples with a calibrated light microscope (Leitz Laborlux S). The thickness measurement before ablation was done in contact with the corneas by measuring perpendicular to their surface. The pachymeter detects the running time of an ultrasonic wave, which is sent through the cornea and reflected on the back side of it. The correction factors resulting from our double measurements ranged between 1.26 and 1.99. They were calculated for each section prepared. Therefore the size in Fig-

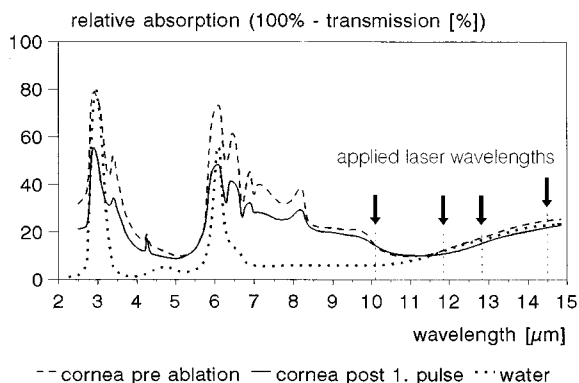


Fig. 2 Absorption of cornea surface layer before and after first pulse and water absorption in the wavelength range from 2.5 to 15 μm .

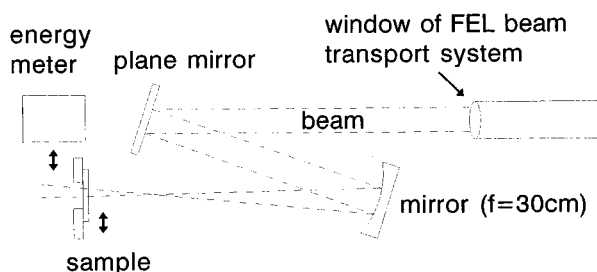


Fig. 3 Experimental setup using the free-electron laser FELIX at FOM.⁶ Beam diameter is about 0.5 mm on the sample.

ures 4 to 7 is not the real size as in a normal hydrated cornea before histologic preparation.

The corneal disks were excised immediately after ablation and fixed in 5% formol. The extent of the collateral thermal damage was assessed histologically by hematoxylin and eosin (H&E) staining and 12 to 22 cross sections (5 to 6 μm thickness) on each laser spot. With the calibrated light microscope, several measurements (10 to 20) were made at the bottom of the crater. Twenty-four craters were evaluated for each wavelength. The experimental data were compared with theoretical calculations according to the *continuous*⁸ and the *blow-off* ablation models.^{9,4,10}

3 ABLATION MODELS

3.1 CONTINUOUS ABLATION MODEL

The continuous ablation model is based upon:

- Lambert's law,
- constant energy per square unit,
- one-dimensional calculation,
- ablation as solely the result of vaporization, and
- disregard of heat conduction.

Heat conduction is disregarded because the thermal diffusivity of the tissue is so small that the thermal relaxation time is up to two orders of magnitude higher than the pulse duration used at FELIX. The thermal relaxation time is about 400 μs at a penetration depth of 14 μm (CO₂ laser)¹¹ and about 20 μs for the minimal penetration depth used at FELIX (14.5 μm wavelength). Therefore minimal heat conduction was achieved with the FELIX pulse length.

The wavelengths we investigated were between 10.1 and 14.5 μm ; therefore the penetration depth of the laser light in the tissue was between 2.5 and 15 μm . The distance of the collagen layers is about 63 nm¹² (67 nm¹³). Therefore we think that the corneal stroma appears homogeneous with the electromagnetic wave.

According to Lambert's law, energy density decreases with increasing depth in the cornea. The energy deposited in the corneal tissue beneath the

bottom of the ablation crater, where the energy density is not sufficient for ablation, is thus not available for ablation. This energy is absorbed by the remaining tissue. In the following equation it is defined by E_R . This energy causes the thermal collateral damage.

$$E_R = \int_0^{\infty} e_V A \exp(-\alpha x) dx \quad \text{or} \quad E_R = e_V A / \alpha, \quad (1)$$

where A is irradiated area, α is the absorption coefficient of the tissue [water⁷ + cornea matrix (Figure 2)], and e_V is the energy density required for vaporization. The variable x is a vertical measurement of depth into the corneal tissue beneath the surface. The heat for vaporizing water of 30°C is 2.428 kJ/g; therefore 2500 mJ/mm³ was taken for e_V .¹⁴

The maximum depth for a temperature T needed to cause coagulation in tissue can be calculated as follows:

$$e_T = e_V e^{-\alpha x}; \quad \text{therefore} \quad x_T = 1/\alpha (\ln e_V / e_T)$$

or x_T is proportional to $1/\alpha$; (2)

thus x_T is proportional to E_R ($E_V, A = \text{const.}$) where e_T is the energy density that is sufficient to reach the temperature T . e_T is calculated with the specific heat of water (4.182 J/(g1°C)),¹⁵ $e_T = (T_1 - T_2) 4.182 \text{ J/(g1°C)} = (168 \text{ mJ/mm}^3)$. Coagulation, an irreversible thermal effect on tissue, takes place above 60°C.¹⁶ The corneas were at room temperature. Therefore a temperature difference of 40°C was taken for $T_1 - T_2$ [T_1 : 60°C; T_2 : 20°C (room temperature)]. The theoretical calculation of the ablation depth is based upon the assumption that the total energy E_{tot} is divided into two parts: the energy absorbed in the remaining tissue, E_R and the energy consumed by vaporization, E_{vap} ($E_{\text{tot}} = E_{\text{vap}} + E_R$).

The ablation process begins when the energy density at the surface is high enough to vaporize tissue water explosively. The vaporization process continues until the end of the pulse. Under this assumption, the energy density at the edge of the ablation zone is constant until the end of the pulse (the value of the energy density is e_V). Therefore, e_V is constant over the whole ablation volume. This leads to

$$\begin{aligned} \text{ablation volume} &= x_V A = E_{\text{vap}} / e_V \\ \text{or} \quad x_V &= E_{\text{vap}} / (e_V A) \end{aligned}$$

Following Eq. (1):

$$\begin{aligned} x_V &= (E_{\text{tot}} - e_V A / \alpha) / (e_V A) = E_{\text{tot}} / (e_V A) - 1/\alpha \\ &= (1/\alpha)(E_{\text{tot}} / E_R - 1). \end{aligned} \quad (3)$$

The profile of the ablation craters can be assumed as a Gaussian (Figures 4 to 7). Therefore a nonconstant energy density (with a Gaussian beam profile) was used: $e(r) = e_0 \exp(-2r^2/w^2)$ (energy density) where r is the radius of the beam, and w is the width of the Gaussian ($w = 0.29 \text{ mm}$ reproduces the craters). According to this assumption, the depth was calculated with $x_V = 2E_{\text{tot}} / (\pi e_V w^2) - 1/\alpha$ (see Appendix).

3.2 BLOW-OFF ABLATION MODEL

The blow-off ablation model is based on the assumption that the ablation process begins after the end of the laser pulse. Therefore, an exponential energy density in the vertical direction into the tissue beneath the surface is expected at the end of the laser pulse. The energy density is attenuated to a value of e_V within the part of the tissue that is ablated. e_V defines this depth. This ablation depth was calculated again with a Gaussian beam profile and the absorption coefficient α of the tissue. Therefore the depth results in: $x_B = 1/\alpha \ln(2E_{\text{tot}}\alpha / (\pi e_V w^2))$ (see Appendix). The values are shown in Table 1.

The calculation of the collateral thermal damage zone is based upon E_R (remaining energy) and therefore the two ablation models do not differ. Calculated and measured values are shown in Table 2.

4 RESULTS

Figures 4 to 7 show the ablation zones at 10.1-, 11.8-, 12.8-, and 14.5 μm wavelengths. The ablation depths in Figures 4 to 6 are 400 to 500 μm . Crater diameters at the surface of the tissue are between 230 and 440 μm . The extension of the thermal damage due to subablative laser intensity at the surface of the corneas is marked in the pictures. It is up to 110 μm on each side of the cross section of the crater at the wavelengths with lower absorption (10.1/11.8 μm). The crater diameters in Figures 4 and 5 are a bit smaller than the mean value of the other 23 craters at each wavelength. In Figure 7 the ablation depth is smaller; about 300 μm . The crater shown is less deep than all the other craters that were measured at the same wavelength. Table 1 shows the ablation depth/pulse (z) determined in the histologic cross sections. The values are between 45 and 50 μm per pulse. The ratio of measured and calculated values (x_V/z) and (x_B/z) determines the prediction accuracy.

The collateral thermal damage (d = extension of eosinophilic zone at the bottom of the incisions) is shown in Table 2. The values are all around 10 to 12 μm . The extension of the collateral thermal damage zone was compared with the calculated values. As in Table 1, the ratio x_T/d determines the prediction accuracy.

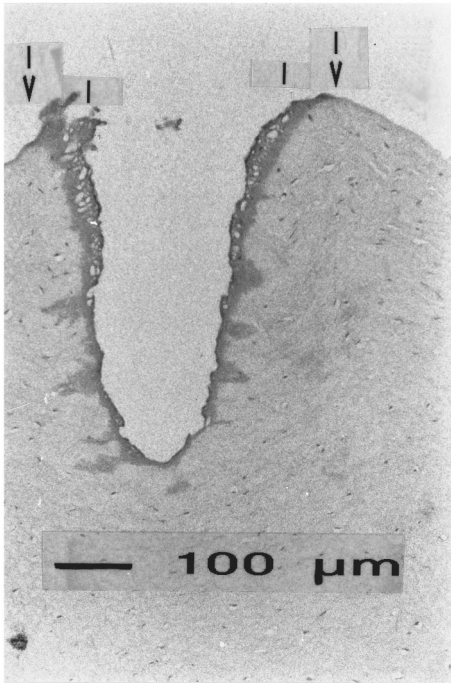


Fig. 4 Ablation zone at 10.1 μm wavelength.

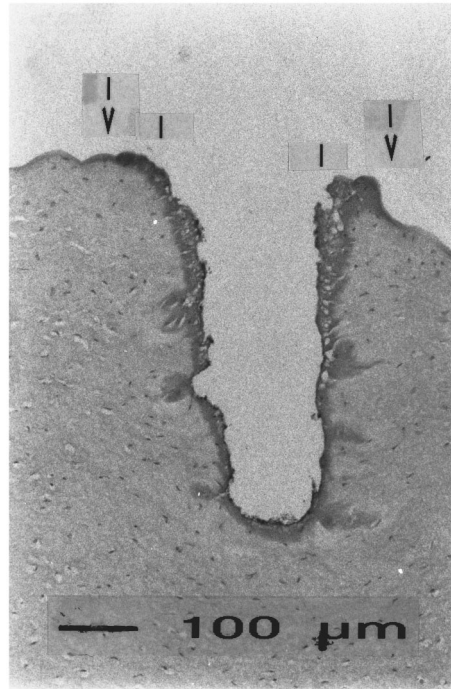


Fig. 5 Ablation zone at 11.8 μm wavelength.

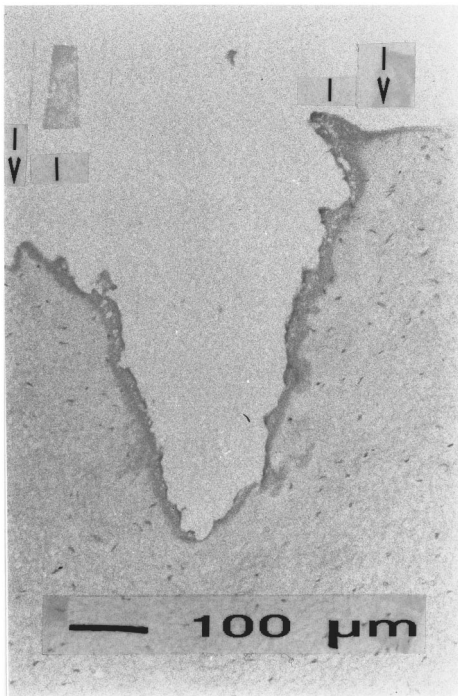


Fig. 6 Ablation zone at 12.8 μm wavelength.

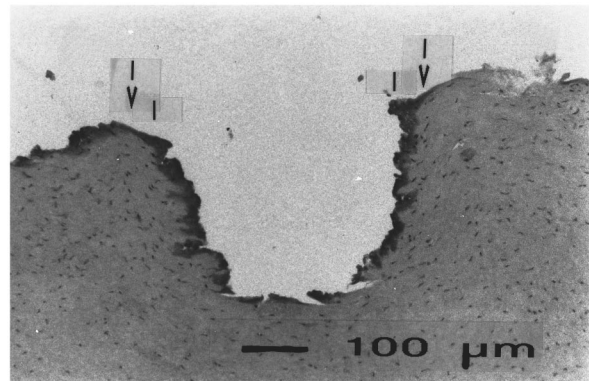


Fig. 7 Ablation zone at 14.5 μm wavelength.

Figs. 4-7 The crater diameters at the surface of the tissue are indicated by vertical lines, and the extension of thermal damage at the surface of the cornea by arrowheads.

Table 1 Ablation depth (*absorption of the cornea matrix was taken into account).

Wavelength (μm)	Measured z ($\mu\text{m}/\text{pulse}$)	Continuous abl. model x_V ($\mu\text{m}/\text{pulse}$)	Quotient x_V/z	Blow-off abl. model x_B ($\mu\text{m}/\text{pulse}$)
10.1	49.4 \pm 6.7	39.0	0.79 \pm 0.12	19.1
10.1*	49.4 \pm 6.7	49.6	1.00 \pm 0.17	10.8
11.8	46.4 \pm 6.0	48	1.03 \pm 0.16	12.2
12.8	47.1 \pm 10.7	46.5	0.99 \pm 0.29	9.4
14.5	45.5 \pm 4.1	44.2	0.97 \pm 0.10	8.3

5 DISCUSSION

These first ablation experiments in corneas carried out at FELIX in the wavelength range from 10.1 μm to 14.5 μm demonstrate that an effective ablation of cornea (an example of biological tissue with high water content) can be obtained in this wavelength range. In the wavelength range from 11.8 to 14.5 μm , the water absorption coefficient α dominates the absorption of the material (Figure 2). At the 10.1 μm wavelength, the absorption seems to be dominated by water and the matrix of the cornea. The cornea components contain glucose, galactose, and mannose, as well as other elements of the collagen matrix, which all have molecule endings $-\text{CH}-\text{OH}_2$ absorbing strongly at around 10 μm wavelength. Therefore the "right" ablation depth/pulse could not be calculated exclusively using the absorption coefficient of water alone. The same absorption coefficient as that at 12.4 μm wavelength was used to calculate the ablation depth/pulse and the thermal collateral damage at 10.1 μm . This was done because the absorption at 10.1 μm is as high as that at 12.4 μm (Figure 2). To calculate the absolute ablation depth with the model presented, based upon α and a continuous ablation process, the ablation craters were assumed to be Gaussian. As a result, the ratio calculated for a measured ablation rate (x_V/z) is nearly constant and the mea-

sured values can be described well by the theoretical calculations, which are based upon α and a continuous ablation process.

The ablation depth reached in our experiments is much greater than the ablation depth expected from the calculations based upon the blow-off ablation model. Especially at a high absorption coefficient, the values differ by a factor of about 5. Assuming a greater penetration depth in the tissue (e.g., as in Ref. 17), the ablation depth calculated with the blow-off model increases by up to a factor of about 2. The blow-off ablation model, which describes ablation with UV wavelengths at short pulse lengths very well,¹⁸ is assumed to be unsuitable for the IR ablation process at a pulse length on the order of microseconds or longer based upon the water absorption coefficient α .

The collateral damage at the bottom of the incisions after ablation is on the same order as the collateral damage inflicted at 3 and 6 μm with an FEL¹⁹ and increases with a decreasing absorption coefficient. The extension of the thermal damage zone was found to be on the same order in measurement and calculation.

It is shown that in the mid-IR wavelength range between 11.8 and 14.5 μm the absorption of laser light in corneal tissue is mostly based upon water. At 10.1 μm , the low water absorbance leads to an increase in the importance of other absorbers inside the tissue besides water. In the wavelength range investigated, the absorption coefficient of water is much higher than the absorption coefficient of the total of all other absorbers inside the tissue, except at wavelengths below 11.5 μm .

We made an estimate for the absorption coefficient α of the corneal tissue from spectroscopic data (Figure 2) at a 10.1- μm wavelength. Other effects play a minor role in that wavelength range. A small absorption shift to shorter wavelength during ablation due to heating does not result in a remarkable shift of absorption because in the wavelength range investigated there are no large changes in tissue absorption. Our model does not account for a part of the laser pulse that might be scattered or blocked

Table 2 Collateral thermal damage.

Wavelength (μm)	Measured d (μm)	Abl. model x_T (μm)	Quotient x_T/d
10.1	12.4 \pm 1.8	40.3	3.3 \pm 0.6
10.1*	12.4 \pm 1.8	11.5	0.9 \pm 0.2
11.8	12.1 \pm 2.8	14.4	1.2 \pm 0.3
12.8	10.9 \pm 2.2	9.6	0.9 \pm 0.2
14.5	9.6 \pm 1.1	8.1	0.8 \pm 0.1

by ablation particles. It ignores photoacoustic effects. Nevertheless, all these effects do have an effect on the fluence. According to our measurements, these effects are within our measured error bars. However, we do know that there might be an error in estimating the fluence because the pulse-to-pulse stability of the FEL and the spot size determination provide the possibility of incorrect values.

It is shown conclusively that the continuous model can predict the ablation depth in water-containing tissue if the absorption coefficient α is known. The very simple ablation model, which does not describe the tissue properties correctly (e.g., the tissue matrix), correlates surprisingly well with the experimental data.

With this knowledge, clinical applications for IR lasers at pulse lengths in the range of microseconds or longer (no plasma-induced ablation) can be designed better. The knowledge of the water content of the tissue and the applied wavelength (or absorption coefficient) together with the fluence, make it possible to predict the ablation efficiency. Or in other words, the laser-tissue interactions that are desired, such as coagulation and ablation together with ablation depth, can be adjusted better. As a result, a wavelength-tunable FEL is a valuable tool for performing ablation experiments with laser wavelengths that are not available from other laser sources.

Acknowledgment

The authors are indebted to Prof. M. J. van der Wiel and Dr. P. W. van Amersfoort for valuable advice and their operation of the free-electron laser. M. Ostertag acknowledges a grant from the Alexander von Humboldt Stiftung. This work received support from the European Union through Human Capital and Mobility, and the U.S. Office of Naval Research Grant 00014-91-0109, subcontract 11061 S6.

6 APPENDIX

6.1 CONTINUOUS ABLATION MODEL

The ablation depth x_V can be calculated by $E_R = e_V A / \alpha$ [Eq. (1)].

It follows that $E_{\text{tot}} = e_0 A / \alpha$ or $e_0 / \alpha = E_{\text{tot}} / A$ and E_{tot} / A is the same as I_0 , therefore

$$e_0 / \alpha = E_{\text{tot}} / A = I_0. \quad (4)$$

Together with $x_V = (1/\alpha)(E_{\text{tot}}/E_R - 1)$ [Eq. (3)], it follows that

$$x_V = (1/\alpha)(e_0/e_V - 1). \quad (5)$$

Assuming a Gaussian energy density $e_0(r) = e_0 \exp(-2r^2/w^2)$ (Gaussian beam profile), $x(r)$ is calculated by

$$I(r, \Phi, x) = E_{\text{tot}} g(r, \Phi) \exp(-\alpha x);$$

$$\text{with } \int g(r, \Phi) r dr d\Phi = 1. \quad (6)$$

$I(r) = I_0 \exp(-2r^2/w^2) = E_{\text{tot}} g(r)$ following $g(r) = I_0 / E_{\text{tot}} \exp(-2r^2/w^2)$. $g(r) = g(r, \Phi)$ and $g(r)$ set in (6) results in: $1 = (I_0 / E_{\text{tot}}) \pi w^2 / 2$ or $I_0 = 2E_{\text{tot}} / (\pi w^2)$. Therefore, x_V can be calculated with Eqs. (4) and (5): $x_V = 2E_{\text{tot}} / (\pi w^2 e_V) - 1/\alpha$.

6.2 BLOW-OFF ABLATION MODEL

The ablation depth x_B can be calculated by

$$E_{\text{vap}} = E_{\text{tot}} - E_R = \int_0^x e_V A \exp(\alpha z) dz$$

$$= (e_V A / \alpha) (\exp(\alpha x) - 1)$$

$$\text{Thus } x_B = (1/\alpha) \ln(E_{\text{vap}} / E_R + 1), \quad (7)$$

Taking into account $E_R = e_V A / \alpha$ [Eq. (1)] and assuming a Gaussian beam profile, the depth results in $x_B = (1/\alpha) \ln(e_0/e_V)$ [Eq. (7)] following from Eqs. (3) and (4),

$$x_B = (1/\alpha) \ln(2E_{\text{tot}} \alpha) / (\pi w^2 e_V).$$

REFERENCES

1. R. L. McCally, R. A. Farrell, and C. B. Barger, "Cornea epithelial damage exposed to Tm:YAG laser radiation at 2.02 μm ," *Lasers Surg. Med.* **12**, 598-603 (1992).
2. T. Bende, M. Kriegerowski, and T. Seiler, "Photoablation in different ocular tissues performed with an Erbium: YAG laser," *Lasers Light Ophthalmol.* **2** (4), 263-269 (1989).
3. O. Kermani, H. Lubatschowski, Th. Assauer, W. Ertmer, A. Lukin, B. Ermakov, and G. K. Krieglstein, "Q-switched CTE:YAG (2.69 μm) laser ablation: basic investigations on soft (corneal) and hard (dental) tissues," *Lasers Surg. Med.* **13**, 537-542 (1993).
4. Q. Ren, V. Venugpalan, K. Schomaker, T. F. Deutsch, T. F. Flotte, C. A. Puliafito, and R. Birngruber, "Mid-infrared laser ablation of the cornea: a comparative study," *Laser Surg. Med.* **12**, 274-281 (1992).
5. J. T. Walsh Jr. and T. F. Deutsch, "Pulsed CO₂ laser tissue ablation: measurement of the ablation rate," *Lasers Surg. Med.* **8**, 264-275 (1988).
6. D. Oepts, A. F. G. van der Meer, and P. W. van Amersfoort, "The free-electron laser user facility FELIX," *Infrared Phys. Technol.* **36**, 297-308 (1995).
7. G. M. Hale and M. R. Querry, "Optical constants of water in the 200 nm to 200 μm wavelength region," *Appl. Opt.* **12** (3), 555-563 (1973).
8. V. Srinivasan, Mark A. Smrtic, and S. V. Babu, "Excimer laser etching of polymers," *J. Appl. Phys.* **59** (11), 3861-3867 (1986).
9. M. Ostertag, R. Walker, T. Bende, and B. Jean, "Optimizing photoablation parameters in the mid IR: a predictive model for the description of experimental data," *Proc. SPIE* **2391**, 138-149 (1995).
10. A. McKenzie, "How far does thermal damage extend beneath the surface of CO₂ laser incisions?" *Phys. Med. Biol.* **28** (8), 905-912 (1983).
11. J. T. Walsh Jr., T. J. Flotte, R. R. Anderson, and T. F. Deutsch, "Pulsed CO₂ laser tissue ablation: effect of tissue type and pulse duration on thermal damage," *Lasers Surg. Med.* **8**, 108-118 (1988).

12. N. S. Malik, S. J. Moss, N. Ahmed, A. J. Furth, R. S. Wall and K. M. Meek, "Ageing of human corneal stroma: structural and biochemical changes," *Biochim. Biophys. Acta* **1138**, 222–228 (1992).
13. J. E. Scott and M. Haigh, "Small proteoglycan–collagen interactions: keratan sulphate proteoglycan associates with rabbit corneal fibrils at the 'a' and 'c' bands," *Biosci. Rep.* **5**, 765–774 (1985).
14. H. Sieber, *Mathematische Tafeln*, p. 127, Verlag Ernst Klett, Stuttgart (1979).
15. F. Dorn and F. Bader, *Physik Oberstufe Band M*, p. 231, Verlag Herrmann Schroedel, Hanover (1975).
16. G. J. Müller and B. Schaldach, "Basic laser tissue interaction, safety and laser tissue interaction," in *Advances in Laser Medicine*, H.-P. Berlien and G. J. Müller, Eds., Vol. II, pp. 17–25, Ecomed Verlag, Landsberg (1989).
17. T. Seiler and J. Wollensak, "Fundamental mode photoablation of cornea for myopic correction: 1. Theoretical background," *Lasers Light Ophthalmol.* **5** (4), 199–203 (1993).
18. R. Srinivasan, "Application of infrared and ultraviolet lasers to the cornea II," *Dynamics of the Ultraviolet Laser Ablation of Corneal Tissue, Laser Technology in Ophthalmology*, Marshall, Ed., Chap 1, pp. 215–220, Kugler & Ghedini Amsterdam (1988).
19. T. Bende, R. Walker, and B. Jean, "Thermal collateral damage in porcine corneas after photoablation with free electron laser," *Refr. Corn. Surg.* **11** (2), 129–136 (1995).